AGU PUBLICATIONS

Geophysical Research Letters

RESEARCH LETTER

10.1002/2016GL072345

Key Points:

- Dust record based on ^{4}He flux from the Subarctic North Pacific covering the last 170,000 years
- Periods of higher dust flux correlate with reduced summer insolation at subarctic latitudes
- Increased dust supply inferred to reflect dust season expansion into summer and fall in East Asia

Supporting Information:

- Supporting Information S1
- Data Set S1

Correspondence to:
S. Serno,
s.serno@qub.ac.uk

Citation:
Serno, S., G. Winckler, R. F. Anderson, S. L. Jaccard, S. S. Kienast, and G. H. Haug (2017), Change in dust seasonality as the primary driver for orbital-scale dust storm variability in East Asia, *Geophys. Res. Lett.*, *44*, doi:10.1002/2016GL072345.

Received 14 DEC 2016
Accepted 3 MAR 2017
Accepted article online 15 MAR 2017

Change in dust seasonality as the primary driver for orbital-scale dust storm variability in East Asia

Sascha Serno[1,2,3], Gisela Winckler[1,4], Robert F. Anderson[1,4], Samuel L. Jaccard[5], Stephanie S. Kienast[6], and Gerald H. Haug[7,8]

[1]Lamont-Doherty Earth Observatory, Columbia University, Palisades, New York, USA, [2]DFG-Leibniz Center for Surface Process and Climate Studies, Institute of Earth and Environmental Science, University of Potsdam, Potsdam, Germany, [3]Now at School of Mechanical and Aerospace Engineering, Queen's University of Belfast, Belfast, UK, [4]Department of Earth and Environmental Sciences, Columbia University, New York, New York, USA, [5]Institute of Geological Sciences and Oeschger Center for Climate Change Research, University of Bern, Bern, Switzerland, [6]Department of Oceanography, Dalhousie University, Halifax, Nova Scotia, Canada, [7]Geological Institute, ETH Zurich, Zurich, Switzerland, [8]Now at Climate Geochemistry Department, Max Planck Institute for Chemistry, Mainz, Germany

Abstract Glacial periods are recognized to be dustier than interglacials, but the conditions leading to greater dust mobilization are poorly defined. Here we present a new high-resolution dust record based on ^{230}Th-normalized ^{4}He flux from Ocean Drilling Program site 882 in the Subarctic North Pacific covering the last 170,000 years. By analogy with modern relationships, we infer the mechanisms controlling orbital-scale dust storm variability in East Asia. We propose that orbital-scale dust flux variability is the result of an expansion of the dust season into summer, in addition to more intense dust storms during spring and fall. The primary drivers influencing dust flux include summer insolation at subarctic latitudes and variable Siberian alpine glaciation, which together control the cold air reservoir in Siberia. Changes in the extent of the Northern Hemisphere ice sheets may be a secondary control.

1. Introduction

Eolian dust is a major driving factor in the climate system through its influence on light scattering and absorption [*Tegen and Fung*, 1994], cloud properties [*Kaufman et al.*, 2002], and ice/snow albedo [*Painter et al.*, 2010]. Dust also influences the oceanic carbon cycle by delivering micronutrients like iron [*Jickells et al.*, 2005]. Paleorecords of dust can be used to reconstruct climate conditions in the source regions and atmospheric transport patterns [*Nagashima et al.*, 2007; *Serno et al.*, 2015].

The East Asian deserts are the second largest global dust source [*Ginoux et al.*, 2004]. Some of these source regions, the Taklimakan desert and deserts in Inner Mongolia (Badain Jaran, Tengger, and Mu Us), are the dominant dust sources for both the Subarctic North Pacific (SNP) [*Sun et al.*, 2001; *Serno et al.*, 2014] and Greenland [*Biscaye et al.*, 1997; *Bory et al.*, 2003]. While the modern processes controlling dust outbreaks in these source regions and atmospheric transport around the Northern Hemisphere (NH) are relatively well understood, much less is known about their orbital-scale variability. This is mainly due to the scarcity of well-resolved records from the SNP covering multiple climatic cycles. Previous studies found cold stadials during the last glacial period to be dustier in East Asia [*Porter and An*, 1995; *Xiao et al.*, 1999; *Nagashima et al.*, 2007, 2011], suggesting a link between North Atlantic climate events and East Asian dust storm frequency. However, the exact mechanisms behind dust variability over longer timescales are still uncertain. Because of the importance of dust in the climate system, understanding the factors driving dust flux changes over different timescales provides a benchmark to test models used to predict changes in atmospheric circulation patterns and dust transport and deposition. Here we present a new high-resolution dust flux record for the last 170,000 years from Ocean Drilling Program (ODP) site 882 (50.4°N, 167.6°E, 3244 m water depth) (Figure 1).

2. Methods

We used a modified age-depth relationship for ODP 882 (details in Text S1 in the supporting information), building on previous work by *Jaccard et al.* [2005, 2009], *Galbraith et al.* [2007], and *Keigwin* [1998]. For the last 33,000 years we use the age model of *Galbraith et al.* [2007]. For the period from 33,000 to

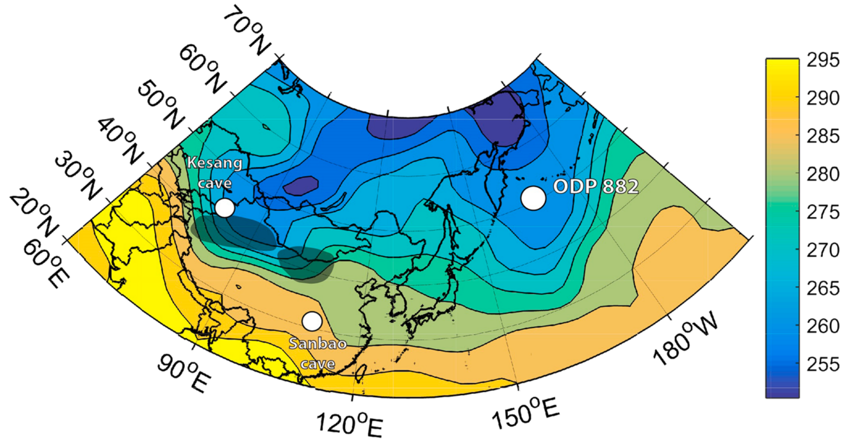

Figure 1. The 850 mb air temperature (in Kelvin) in East Asia on 7 April 2001 from the NCEP-NCAR Reanalysis [*Kalnay et al.*, 1996]. Shaded black areas indicate the dominant East Asian dust source regions for long-range transport. The map shows a cold air outbreak from Siberia over the desert regions in northern China and Mongolia, resulting in one of the largest dust storms in recent decades on 6–9 April 2001 [*Liu et al.*, 2003]. White points indicate the location of ODP site 882 and East Asian speleothem records from the Kesang and Sanbao Caves cited in the manuscript.

~180,000 years B.P. (before present to 1950), we tied the ODP 882 Ca/Al record [*Jaccard et al.*, 2005, 2009] to well-dated calcite preservation records from the Subantarctic Atlantic [*Peterson and Prell*, 1985; *Bassinot et al.*, 1994; *Hodell et al.*, 2001, 2003; *Sachs and Anderson*, 2005; *Anderson et al.*, 2008; *Barker and Diz*, 2014] (Figures S1 and S2 and Table S1).

Our record is based on ^{230}Th-normalized terrigenous ^{4}He ($^4He_{terr}$) flux. Details of the analytical methods [*Choi et al.*, 2001; *Fleisher and Anderson*, 2003; *Francois et al.*, 2004; *Winckler et al.*, 2005; *Serno et al.*, 2014] and the particle-size distribution [*McGee et al.*, 2013; *Bista et al.*, 2016] are provided in Text S2. High ^{4}He concentrations in dust and negligible concentrations in volcanics make $^4He_{terr}$ a particularly useful dust proxy for the SNP where large lithogenic inputs other than dust (e.g., volcanics) contribute to sediments [*Patterson et al.*, 1999; *Winckler et al.*, 2008; *Serno et al.*, 2014, 2015]. Variability in $^4He_{terr}$ flux at ODP site 882 represents changes in East Asian dust storm activity and dust transport to the SNP (see Text S3 and Figures S3 and S4 for more information [*Jaccard et al.*, 2005, 2009, 2010; *Serno et al.*, 2014; *McGee et al.*, 2016]). Dust flux based on $^4He_{terr}$ is calculated by dividing $^4He_{terr}$ flux by the average East Asian dust endmember $^4He_{terr}$ concentration of 2279 ± 515 (1σ) ncc STP g^{-1} (nano cubic centimeter at standard temperature and pressure per gram).

3. Results and Discussion

3.1. Orbital-Scale Dust Flux Variability in the Subarctic North Pacific

Our dust flux record based on $^4He_{terr}$ is the first high-resolution record from the SNP that applies a novel geochemical fingerprinting technique to deconvolve the sedimentary dust fraction, in combination with ^{230}Th normalization to derive reliable dust flux estimates for the last 170,000 years. The record points to high dust input (>600 mg/cm^2/kyr) during cold periods (Figures 2a and 2b), including the last and penultimate glacial maxima (Marine Isotope Stages, MIS 2 and MIS 6, respectively), as well as dust peaks (>900 mg/cm^2/kyr) during MIS 4 and MIS 5d. Lowest dust fluxes (<400 mg/cm^2/kyr) characterize the last and present interglacial, MIS 5e and MIS 1, respectively, and MIS 5a and MIS 5c. MIS 3 shows dust fluxes only slightly lower than MIS 2. Acknowledging potential uncertainties related to the wide range of East Asian dust endmember $^4He_{terr}$ concentrations (Text S3 and Figure S3), providing these dust flux estimates in addition to the $^4He_{terr}$ fluxes, facilitates comparisons to other studies. Note that the minimal values in MIS 1 agree well with other observational and modeling studies [*Albani et al.*, 2015; *Kienast et al.*, 2016].

The most distinct features of the dust flux record are the large dust peaks during MIS 4 and MIS 5d, with dust fluxes ~1.5 to 2 times higher than during MIS 2 and MIS 6, which are similar to one another. The majority of published dust flux records from the SNP and the Chinese Loess Plateau (CLP) near the East Asian dust

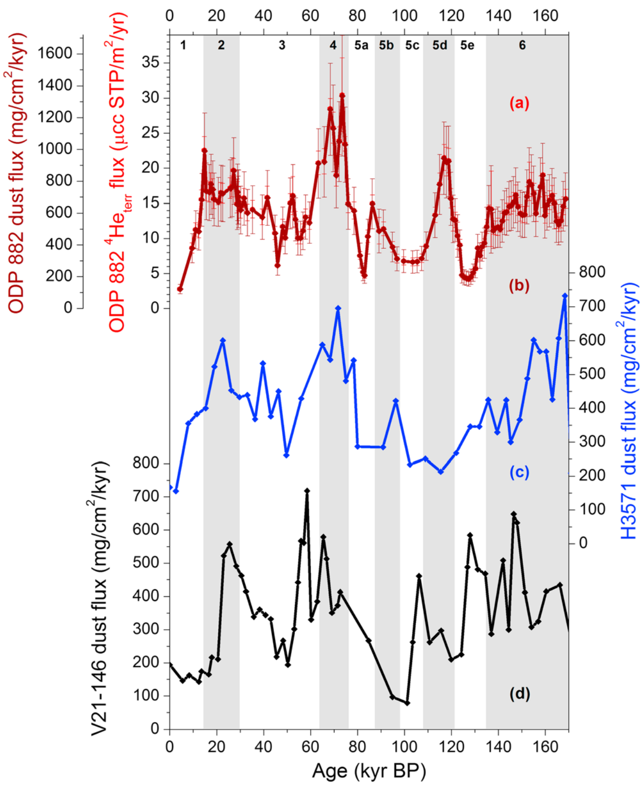

Figure 2. Comparison of different SNP dust records. (a) The ^{230}Th-normalized $^{4}He_{terr}$ flux and (b) dust flux records from ODP site 882, plotted with error bars representing 1σ uncertainties or replicate reproducibility. (c) The mineral dust flux record from core H3571 on Hess Rise (34.9°N, 179.7°E, 3571 m water depth) [*Kawahata et al*., 2000]. (d) Dust accumulation rates from V21-146 on Shatsky Rise (37.7°N, 163.0°E, 3968 m water depth) [*Hovan et al*., 1991]. Gray bars represent the timing of cold intervals, MIS 2, MIS 4, MIS 5b, MIS 5d, and MIS 6.

sources also show a prominent MIS 4 signal (Figures 2c and 2d). More details about CLP dust flux records and their comparability to SNP dust flux records are provided in Text S4 [*Bowler et al*., 1987; *An et al*., 1991, 2014; *Beer et al*., 1993; *Xiao et al*., 1999; *Porter*, 2001; *Kohfeld and Harrison*, 2003; *Sun et al*., 2003, 2006, 2008; *Stevens et al*., 2006, 2013; *Chen et al*., 2007; *Jiang et al*., 2007; *Prins et al*., 2007; *Maher et al*., 2009; *Stevens and Lu*, 2009; *Hao et al*., 2010; *Qiang et al*., 2010; *Kapp et al*., 2011; *Pullen et al*., 2011; *Yang et al*., 2014; *Kang et al*., 2015; *Niu et al*., 2015; *Li et al*., 2016; *Licht et al*., 2016].

However, no study observed a pronounced dust flux maximum during MIS 5d. The SNP records rather show high dust accumulation rates during MIS 5e and MIS 5c [*Hovan et al*., 1991] or MIS 5c to MIS 5b [*Kawahata et al*., 2000]. Similarly, a record of dust concentrations from the western SNP, based on trace element concentrations in marine sediments and endmember values in Chinese loess and Kurile-Kamchatka volcanics, shows a prominent dust concentration peak during MIS 5c [*Shigemitsu et al*., 2007]. All existing records from the SNP may be prone to large uncertainties in their eolian dust reconstructions due to age model uncertainties, poor or missing characterization of mass accumulation rates, and uncertainties in their discrimination of eolian dust from the total lithogenic fraction in the sediments. It seems plausible that minor adjustments to the age models of published dust flux records by up to 10,000 years due to age model uncertainties, in addition to the consideration of potential uncertainties in the reconstructed dust fluxes, would make the different records consistent and cause them to show a very similar variability during the last 170,000 years (Figure 2).

3.2. Potential Driving Factors for Dust Flux Changes in the Subarctic North Pacific

The observed dust flux changes at ODP 882 may be the result of different factors: changes in (a) East Asian dust storm seasonality, (b) dust transport, or (c) size of the dust source areas. We do not expect the ODP 882 record to reflect shifts in the spatial pattern of dust deposition in the SNP for two reasons: First, the modern spatial dust pattern in the SNP is fairly uniform [*Serno et al*., 2014], so dust flux at ODP 882 is not expected to be sensitive to a large-scale shift of the dust plume. Second, more intense dust mobilization in East Asia should result in a more southerly location of the westerly core zone over a longer period of the year (section 3.3). Therefore, higher dust mobilization in East Asia during MIS 5d should result in higher dust fluxes in the southern compared to the northern SNP, opposite to the observed trend in SNP records (Figure 2). Consequently, we exclude shifts in the pattern of dust deposition to explain ODP 882 dust flux variability.

Alternative driving factors for glacial-interglacial dust flux variability are wind gustiness and expansion of the dust source areas [*McGee et al*., 2010]. Expanded closed-basin lakes near the Taklimakan and Inner Mongolian deserts are observed during dustier time intervals of the last glacial period [e.g., *Chen and Bowler*, 1986; *Ma et al*., 2004; *Yang et al*., 2011]. In particular, several lakes from near the Taklimakan desert show high lake stands during MIS 2 and MIS 4 and high dust periods in ODP 882 [*Ma et al*., 2004]. Consequently, we exclude dust source expansion as a driving factor for dust flux variability observed at ODP site 882 and focus on the influence of changes in dust storm seasonality.

3.3. Modern Processes Controlling Seasonal Dust Storm Changes in East Asia

Knowledge of the modern processes controlling seasonal dust storms provides a basis for interpreting past dust flux variability. We follow the argumentation of *Roe* [2009] to discuss the modern dust storm seasonality in East Asia. Today, climatological data demonstrate that East Asian dust outbreaks are almost exclusively springtime phenomena [e.g., *Qian et al*., 2002; *Kurosaki and Mikami*, 2005], when the increasing meridional temperature gradient between low and high latitudes and cyclogenesis lead to conditions that intensify dust storm activity [*Roe*, 2009].

3.3.1. Winter

During wintertime, the middle-to-upper tropospheric horizontal westerly jet is displaced to the south of the Tibetan Plateau [*Hoskins and Hodges*, 2002; *Schiemann et al*., 2009], and due to a persistent Siberian high-pressure system, there is an almost complete absence of dust-mobilizing cyclogenesis in East Asia.

3.3.2. Spring

During spring, Siberia is still covered in snow and remains cold, while subtropical landmasses warm up quickly. The Siberian High is much weaker, resulting in the atmosphere being less stable to vertical displacement [*Roe*, 2009]. The region of strongest horizontal westerly wind spreads farther northward over the Tibetan Plateau compared to winter, although its core axis remains in its wintertime position south of the Tibetan Plateau [*Schiemann et al*., 2009]. These two factors result in higher interaction of the upper level waves, propagating with the westerly jet, with the land surface to produce cyclones in the desert regions [*Roe*, 2009].

During the synoptic development of midlatitude storms, the cold air residing in Siberia is advected southeastward over the deserts [*Roe*, 2009] (Figure 1). The intense temperature gradients across these fronts, a result of the strong meridional temperature gradient, produce significant vertical wind displacements that draw strong winds close to the land surface. Furthermore, the enhanced vertical wind shear and mixing produce near-surface convection that leads to strong surface wind gusts during the passage of these cold frontal systems [e.g., *Wallace and Hobbs*, 2006; *Roe*, 2009]. The wind gusts lift dust above 5000 m altitude where the dust is transported around the NH by the prevailing westerly jet [*Sun et al*., 2001]. In addition to cold fronts, mountain airflow dynamics may also play a role in the generation of dust storms in this region, with atmospheric flow over and past the high topography stretching vertical air masses and imparting a curvature to the circulation that tends to favor cyclone development [*Roe*, 2009].

3.3.3. Summer

The Siberian High is absent during summer, and the subarctic latitudes are warmer compared to spring, which leads to a reduced meridional temperature gradient and unfavorable conditions for wind gustiness in the desert regions [*Roe*, 2009]. Higher precipitation in central China associated with the East Asian Summer Monsoon (EASM) [*Sampe and Xie*, 2010] likely suppresses dust mobilization further.

3.3.4. Fall

The Siberian High is just slightly stronger during fall compared to spring, and the meridional temperature gradient is similar [*Roe*, 2009]. However, the location of the coldest air mass is displaced eastward of the dust source regions during fall compared to spring, driven by differences in sea ice extent in the Barents Sea, which influences snow cover and temperatures in Siberia. This results in less intense dust mobilization during fall compared to spring [*Roe*, 2009].

3.4. Influence of Seasonal Insolation Changes

We hypothesize that the orbital-scale changes in dust flux in the SNP may be explained by changes in dust storm seasonality in East Asia. As discussed in section 3.3, modern East Asian dust seasonality, with a majority of dust storms occurring during spring, is driven by seasonal changes in the meridional temperature gradient and cyclogenesis. Sufficiently reliable paleotemperature records from subarctic and subtropical latitudes in East Asia covering the time interval of interest are not yet available to reconstruct temperature gradients that would have been favorable to cyclogenesis (see Text S5 and Figure S5

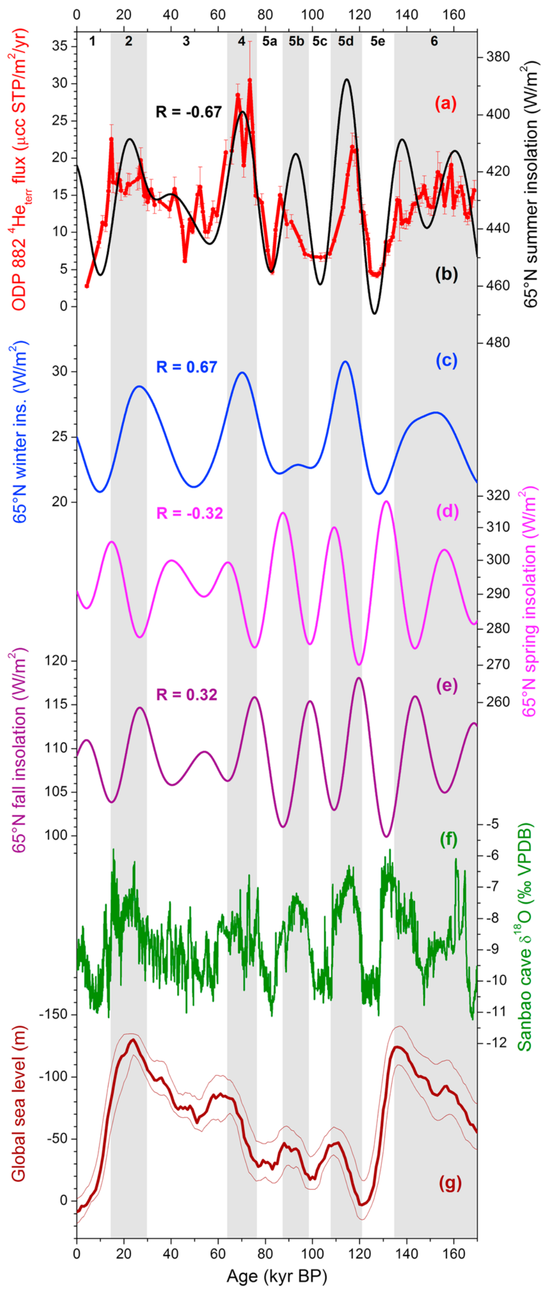

Figure 3. (a) ^{230}Th-normalized ^{4}He$_{terr}$ flux record from ODP 882. Error bars represent 1σ uncertainties or replicate reproducibility. Mean 65°N insolation during (b) summer, (c) winter, (d) spring, and (e) fall, with data from *Paillard et al.* [1996] and calculated from astronomical and insolation time series published by *Berger* [1978]. Pearson correlation coefficients in Figures 3b–3e are for the comparison between the ^{4}He$_{terr}$ flux data from ODP 882 and each seasonal 65°N insolation interpolated for the calendar ages with available ODP 882 dust flux data (see Figure S6). (f) Composite δ^{18}O speleothem record from Sanbao cave, with lower values indicating increased EASM rainfall [*Cheng et al.*, 2016]. (g) Global mean sea level stack, scaled to a value of 0 m at 5 kyr B.P. [*Spratt and Lisiecki*, 2016]. The stacked curve is the PC1 from a principal component analysis on seven global records for a 430–0 kyr window, explaining 83% of the data variance. The thin lines represent the standard deviations of high and low stand estimates across the records. Gray bars represent the cold intervals MIS 2, MIS 4, MIS 5b, MIS 5d, and MIS 6.

for a detailed description of available paleotemperature records [*Thompson et al.*, 1997; *Yao et al.*, 1997; *Prokopenko et al.*, 2001, 2006; *Yang et al.*, 2006; *Melles et al.*, 2012]). *Krinner et al.* [2011] suggested that Siberian summer temperatures are governed to a large degree by insolation, so we will use mean subarctic (65°N) insolation data for all seasons to discuss plausible orbital-scale changes in the seasonal development of the meridional temperature gradient that leads to dust storm activity in East Asia.

3.4.1. Winter

We find a positive correlation between SNP dust flux and 65°N winter insolation ($R = 0.67$; Figures 3a and 3c). However, note that the change in winter insolation is very small compared to other seasons, with a maximum amplitude of ~10 W/m^2 (Figures 3b–3d). Furthermore, snow and ice buildup during the winter is expected to cause unfavorable conditions for dust storms, as discussed in section 3.5. Consequently, we conclude that insolation-induced winter temperature changes in Siberia are rather small and are unlikely to influence the temperature gradient during this season over orbital timescales.

3.4.2. Spring and Fall

The 65°N spring and fall insolation data show patterns that are not well correlated with the ODP 882 dust record ($R = -0.32$ and 0.32 for spring and fall, respectively; Figures 3a, 3d, and 3e). The timing of extrema in spring and fall insolation does not match the dust record. For example, maxima in fall insolation precede peak dust fluxes in MIS 4 and MIS 5d, whereas minima occur after peak dust flux. This indicates that changes in subarctic spring and fall insolation and their effects on the dust storm frequency in East Asia cannot explain the dust flux pattern observed at ODP 882.

3.4.3. Summer

The $^4He_{terr}$ flux record shows a significant negative correlation with summer insolation at 65°N ($R = -0.67$; Figures 3a and 3b). The intervals of highest dust flux, MIS 4 and MIS 5d, are characterized by lowest mean subarctic summer insolation during the last 170,000 years. The other periods of high dust flux, MIS 2, MIS 5b, and MIS 6, also show low summer insolation, although not as low as MIS 4 and MIS 5d. The intervals characterized by lowest $^4He_{terr}$ fluxes, MIS 1 and MIS 5e, fall into periods of high summer insolation. Similarly, high subarctic summer insolation during MIS 5a and MIS 5c correlates with relatively low dust fluxes. Therefore, the observed variability in $^4He_{terr}$ flux and 65°N summer insolation suggests an inverse relationship between subarctic summer insolation and dust storm activity in East Asia.

Based on the comparison between ODP 882 dust flux and seasonal insolation, we propose that the main features in the dust flux record over orbital timescales, in particular the maxima during MIS 4 and MIS 5d, and minima during MIS 1 and MIS 5e, are mainly driven by summer insolation at subarctic latitudes. Low summer temperatures associated with low summer insolation allow a more intense reservoir of cold air in Siberia during a greater fraction of the year. By analogy with modern conditions, extending the presence of cold air in Siberia from spring into summer would lengthen the interval with meridional temperature gradients and spatial horizontal westerly wind positioning favorable to cyclogenesis, thereby extending the period of dust storm activity.

Our hypothesis of a significant influence of subarctic summer insolation on the meridional summer temperature gradient and thus dust storm frequency in East Asia is supported by the well-dated and highly resolved speleothem oxygen isotope ($\delta^{18}O$) records. The record from Kesang Cave, located to the northwest of the Taklimakan desert, indicates that changes in summer rainfall $\delta^{18}O$ are controlled by changes in 65°N summer insolation [*Cheng et al*., 2012]. Furthermore, the intensity of summer rainfall reconstructed from eastern Chinese cave records primarily follows changes in subarctic summer insolation [e.g., *Wang et al*., 2008; *Cheng et al*., 2009, 2016; *Jiang et al*., 2016] (Figure 3f). The findings from the cave records have been interpreted to be the result of shifting summertime boundaries between the horizontal westerly wind jet and EASM. A prolonged dust season from spring into summer therefore would be driven by the same climatic factors influencing the intensity and spatial changes in summer rainfall in central and eastern China.

3.5. Influence of Changes in the Siberian Alpine Glaciation

We also have to consider factors other than insolation that can drive changes in the temperature distribution in East Asia. Extensive alpine glaciation in Siberia has been reconstructed for MIS 4 and MIS 5d, using geomorphological and chronological evidence in northeast Russia [e.g., *Stauch and Gualtieri*, 2008; *Krinner et al*., 2011; *Zech et al*., 2011; *Barr and Clark*, 2012] and lithological and biogeochemical evidence from Lake Baikal sediments [*Karabanov et al*., 1998; *Prokopenko et al*., 2002]. A rather small alpine glacial advance has been reconstructed for MIS 2. The gradual decrease in the Siberian alpine glacier mass during the cold intervals over the last 170,000 years has been explained by changes in subarctic summer temperatures. These temperature changes were driven by subarctic summer insolation and changes in the moisture supply from the ice-free areas of the North Atlantic and Arctic Sea due to the moisture-blocking effect of the Fennoscandian Ice Sheet (FIS), which is thought to have become gradually more extensive from MIS 5d to MIS 2 [*Svendsen et al*., 2004]. The presence of extensive alpine glaciers in Siberia during MIS 4 and MIS 5d may have provided a more intense year-round cold air reservoir as a source for cold surges. If so, the further intensification of the Siberian cold air reservoir during the entire year may have resulted in stronger dust storm events during spring, summer, and fall.

It is thought that the intensity of the Siberian High is influenced by diabatic heating anomalies associated with the underlying snow cover in addition to radiative forcing [*Foster et al*., 1983; *Sahsamanoglou et al*., 1991; *Clark and Serreze*, 2000]. Therefore, a larger snow cover in Siberia as a result of more extensive alpine glaciation during MIS 4 and MIS 5d may have resulted in colder air temperatures and a strengthened high-pressure system during wintertime [*Clark and Serreze*, 2000], leading to suppressed winter dust mobilization.

3.6. Influence of the Northern Hemisphere Ice Sheet Variability

The above mentioned mechanisms describe climate conditions that can explain the main features in orbital-scale dust storm variability as inferred from ODP 882. However, they are not sufficient to explain why dust flux during MIS 5b was lower than during MIS 2 and MIS 6, when all three periods were characterized by similar subarctic summer insolation (Figures 3a and 3b). Similarly, our proposed mechanisms cannot explain the relatively high dust fluxes during MIS 3, an interval with higher subarctic summer insolation and less intense Siberian glaciation. The observed changes in dust fluxes, which increase from MIS 5b to MIS 3 but are similar during MIS 2 and MIS 6, are consistent with the reconstructed ice volume of the Laurentide Ice Sheet, with a rather small extent during MIS 5 and largest ice volumes during MIS 2 and MIS 4 and continuously large volumes during MIS 3 [*Marshall et al*., 2002; *Kleman et al*., 2010]. A similar development with increasing volumes over the course of the last glacial period was suggested for the FIS [*Svendsen et al*., 2004].

We use changes in global sea level during the last glacial period (Figure 3g) to reflect the variable extent of the large NH ice sheets [e.g., *Waelbroeck et al*., 2002; *Siddall et al*., 2003; *Spratt and Lisiecki*, 2016]. The relative differences in dust flux between MIS 2, MIS 3, MIS 5b, and MIS 6 described above can be explained by changes in the extent of the large NH ice sheets. This was probably through the ice sheet's influence on atmospheric circulation patterns, sea surface temperatures, and sea ice extent in the North Atlantic and Arctic Oceans [*Ganopolski et al*., 1998; *Clark et al*., 1999]. All three factors influence temperature gradients and wind patterns throughout the NH, resulting in the ice sheets indirectly regulating climate conditions in East Asia.

4. Conclusions

The dust flux data shown here represent the first high-resolution record from the Subarctic North Pacific that combines $^{4}He_{terr}$ geochemical fingerprinting of eolian dust with ^{230}Th normalization to estimate reliable dust fluxes during the last 170,000 years. Our results provide a new crucial benchmark to better constrain the factors regulating dust variability in East Asia. This will be essential to interpret changes in atmospheric circulation when comparing dust flux records from along the transport path of East Asian dust around the Northern Hemisphere.

Over the duration of our 170,000 year record, the supply of dust accumulating in the Subarctic North Pacific is anticorrelated with subarctic summer insolation. The intervals of highest dust flux, during MIS 4 and MIS 5d, coincide with lowest mean subarctic summer insolation. We hypothesize that orbital-scale dust flux variability at ODP site 882 is driven by changes in the length of the dust season in East Asia, in addition to more intense dust storms during spring and fall, compared to today when dust outbreaks in East Asia are almost exclusively springtime phenomena. We postulate that changes in the subarctic summer insolation and variable Siberian alpine glaciation are the driving factors influencing dust storm activity in East Asia. Future research should therefore assess the role of dust season length on dust flux variability and the influence of changes in ice sheets, Siberian alpine glaciation, and insolation variations. This could be achieved by using general circulation model (GCM) simulations with separate experiments assessing variations in ice sheets and insolation. Experiments such as these would be particularly relevant for MIS 5d, which shows large differences in dust flux reconstructions from different records. However, as pointed out by *Roe* [2009], global climate models lack sufficient spatial resolution to represent cold fronts and may not be adequate to capture the process of lee cyclogenesis. New model simulations will be required to test our data-based hypothesis of dust season expansion as a driving factor for dust flux. The lack of reliable East Asian paleotemperature records covering different seasons during the last glacial period further limits our understanding of temporal changes in meridional temperature gradients as a driver of East Asian dust storm seasonality. The paleoclimate community should aim to produce high-resolution temperature records for different seasons across East Asia to better understand orbital-scale changes in the seasonal evolution of the meridional temperature gradient in this region.

Acknowledgments
All data presented in this manuscript are available in Data Set S1. Samples were provided by the ODP, sponsored by the U.S. NSF and participating countries under the management of Joint Oceanographic Institutions, Inc. Financial support for the analytical work came through U.S. NSF grant OCE1060907 to G.W. and R.F.A. and the DFG-Leibniz Center for Surface Process and Climate Studies at the University of Potsdam to G.H.H. We would like to thank Roseanne Schwartz, Marty Fleisher, and Linda Baker at the Lamont-Doherty Earth Observatory, Erin Wilson at Dalhousie University, and Maureen Soon at the University of British Columbia for laboratory support. Discussions with Gerard Roe and comments by three anonymous reviewers helped to substantially improve the manuscript. This is LDEO contribution 8094.

References

Albani, S., et al. (2015), Twelve thousand years of dust: The Holocene global dust cycle constrained by natural archives, *Clim. Past*, *11*(6), 869–903, doi:10.5194/cp-11-869-2015.

An, Z. S., G. Kukla, S. C. Porter, and J. L. Xiao (1991), Late Quaternary dust flow on the Chinese Loess Plateau, *Catena*, *18*(2), 125–132, doi:10.1016/0341-8162(91)90012-M.

An, Z. S., Y. B. Sun, W. J. Zhou, W. G. Liu, X. K. Qiang, X. L. Wang, F. Xian, P. Cheng, and G. S. Burr (2014), Chinese loess and the East Asian monsoon, in *Late Cenozoic Climate Change in Asia*, edited by Z. S. An, pp. 23–143, Springer, Dordrecht, Netherlands.

Anderson, R. F., M. Q. Fleisher, Y. Lao, and G. Winckler (2008), Modern $CaCO_3$ preservation in equatorial Pacific sediments in the context of late-Pleistocene glacial cycles, *Mar. Chem.*, *111*(1–2), 30–46, doi:10.1016/j.marchem.2007.11.011.

Barker, S., and P. Diz (2014), Timing of the descent into the last Ice Age determined by the bipolar seesaw, *Paleoceanography*, *29*, 489–507, doi:10.1002/2014PA002623.

Barr, I. D., and C. D. Clark (2012), Late Quaternary glaciations in Far NE Russia: Combining moraines, topography and chronology to assess regional and global glaciation synchrony, *Quat. Sci. Rev.*, *53*, 72–87, doi:10.1016/j.quascirev.2012.08.004.

Bassinot, F. C., L. Beaufort, E. Vincent, L. D. Labeyrie, F. Rostek, P. J. Müller, X. Quidelleur, and Y. Lancelot (1994), Coarse fraction fluctuations in pelagic carbonate sediments from the tropical Indian Ocean: A 1500-kyr record of carbonate dissolution, *Paleoceanography*, *9*, 579–600, doi:10.1029/94PA00860.

Beer, J., C. D. Shen, F. Heller, T. S. Liu, G. Bonani, D. Beate, M. Suter, and P. W. Kubik (1993), ^{10}Be and magnetic susceptibility in Chinese loess, *Geophys. Res. Lett.*, *20*, 57–60, doi:10.1029/92GL02676.

Berger, A. L. (1978), Long-term variations of caloric insolation resulting from Earth's orbital elements, *Quat. Res.*, *9*(2), 139–167, doi:10.1016/0033-5894(78)90064-9.

Biscaye, P. E., F. E. Grousset, M. Revel, S. Van der Gaast, G. A. Zielinski, A. Vaars, and G. Kukla (1997), Asian provenance of glacial dust (stage 2) in the Greenland Ice Sheet Project 2 Ice Core, Summit, Greenland, *J. Geophys. Res.*, *102*, 26,765–26,781, doi:10.1029/97JC01249.

Bista, D., S. S. Kienast, P. S. Hill, and M. Kienast (2016), Sediment sorting and focusing in the eastern equatorial Pacific, *Mar. Geol.*, *382*, 151–161, doi:10.1016/j.margeo.2016.09.016.

Bory, A. J. M., P. E. Biscaye, and F. E. Grousset (2003), Two distinct seasonal Asian source regions for mineral dust deposited in Greenland (NorthGRIP), *Geophys. Res. Lett.*, *30*(4), 1167, doi:10.1029/2002GL016446.

Bowler, J. M., K. Z. Chen, and B. Y. Yuan (1987), Systematic variations in loess source areas: Evidence from Qaidam and Qinghai basins, western China, in *Aspects of Loess Research*, edited by T. S. Liu, pp. 39–51, China Ocean Press, Beijing.

Chen, J., G. J. Li, J. D. Yang, W. B. Rao, H. Y. Lu, W. Balsam, Y. B. Sun, and J. F. Ji (2007), Nd and Sr isotopic characteristics of Chinese deserts: Implications for the provenances of Asian dust, *Geochim. Cosmochim. Acta*, *71*(15), 3904–3914, doi:10.1016/j.gca.2007.04.033.

Chen, K. Z., and J. M. Bowler (1986), Late Pleistocene evolution of salt lakes in the Qaidam basin, Qinghai province, China, *Palaeogeogr. Palaeoclimatol. Palaeoecol.*, *54*(1–4), 87–104, doi:10.1016/0031-0182(86)90119-7.

Cheng, H., R. L. Edwards, W. S. Broecker, G. H. Denton, X. G. Kong, Y. J. Wang, R. Zhang, and X. F. Wang (2009), Ice age terminations, *Science*, *326*(5950), 248–252, doi:10.1126/science.1177840.

Cheng, H., P. Z. Zhang, C. Spötl, R. L. Edwards, Y. J. Cai, D. Z. Zhang, W. C. Sang, M. Tan, and Z. S. An (2012), The climatic cyclicity in semiarid-arid central Asia over the past 500,000 years, *Geophys. Res. Lett.*, *39*, L01705, doi:10.1029/2011GL050202.

Cheng, H., et al. (2016), The Asian monsoon over the past 640,000 years and ice age terminations, *Nature*, *534*(7609), 640–646, doi:10.1038/nature18591.

Choi, M. S., R. Francois, K. Sims, M. P. Bacon, S. Brown-Leger, A. P. Fleer, L. Ball, D. Schneider, and S. Pichat (2001), Rapid determination of ^{230}Th and ^{231}Pa in seawater by desolvated micro-nebulization Inductively Coupled Plasma magnetic sector mass spectrometry, *Mar. Chem.*, *76*(1–2), 99–112, doi:10.1016/S0304-4203(01)00050-0.

Clark, M. P., and M. C. Serreze (2000), Effects of variations in East Asian snow cover on modulating atmospheric circulation over the North Pacific Ocean, *J. Clim.*, *13*(20), 3700–3710, doi:10.1175/1520-0442(2000)013<3700:EOVIEA>2.0.CO;2.

Clark, P. U., R. B. Alley, and D. Pollard (1999), Northern Hemisphere ice-sheet influences on global climate change, *Science*, *286*(5442), 1104–1111, doi:10.1126/science.286.5442.1104.

Fleisher, M. Q., and R. F. Anderson (2003), Assessing the collection efficiency of Ross Sea sediment traps using ^{230}Th and ^{231}Pa, *Deep Sea Res., Part II*, *50*(3–4), 693–712, doi:10.1016/S0967-0645(02)00591-X.

Foster, J., M. Owe, and A. Rango (1983), Snow cover and temperature relationships in North America and Eurasia, *J. Clim. Appl. Meteorol.*, *22*(3), 460–469, doi:10.1175/1520-0450(1983)022<0460:SCATRI>2.0.CO;2.

Francois, R., M. Frank, M. M. Rutgers van der Loeff, and M. P. Bacon (2004), ^{230}Th normalization: An essential tool for interpreting sedimentary fluxes during the late Quaternary, *Paleoceanography*, *19*, PA1018, doi:10.1029/2003PA000939.

Galbraith, E. D., S. L. Jaccard, T. F. Pedersen, D. M. Sigman, G. H. Haug, M. Cook, J. R. Southon, and R. Francois (2007), Carbon dioxide release from the North Pacific abyss during the last deglaciation, *Nature*, *449*(7164), 890–894, doi:10.1038/nature06227.

Ganopolski, A., S. Rahmstorf, V. Petoukhov, and M. Claussen (1998), Simulation of modern and glacial climates with a coupled global model of intermediate complexity, *Nature*, *391*(6665), 351–356, doi:10.1038/34839.

Ginoux, P., J. M. Prospero, O. Torres, and M. Chin (2004), Long-term simulation of global dust distribution with the GOCART model: Correlation with North Atlantic Oscillation, *Environ. Modell. Software*, *19*(2), 113–128, doi:10.1016/S1364-8152(03)00114-2.

Hao, Q. Z., Z. T. Guo, Y. S. Qiao, B. Xu, and F. Oldfield (2010), Geochemical evidence for the provenance of middle Pleistocene loess deposits in southern China, *Quat. Sci. Rev.*, *29*(23–24), 3317–3326, doi:10.1016/j.quascirev.2010.08.004.

Hodell, D. A., C. D. Charles, and F. J. Sierro (2001), Late Pleistocene evolution of the ocean's carbonate system, *Earth Planet. Sci. Lett.*, *192*(2), 109–124, doi:10.1016/S0012-821X(01)00430-7.

Hodell, D. A., K. A. Venz, C. D. Charles, and U. S. Ninnemann (2003), Pleistocene vertical carbon isotope and carbonate gradients in the South Atlantic sector of the Southern Ocean, *Geochem. Geophys. Geosyst.*, *4*(1), 1004, doi:10.1029/2002GC000367.

Hoskins, B. J., and K. I. Hodges (2002), New perspectives on the Northern Hemisphere winter storm tracks, *J. Atmos. Sci.*, *59*(6), 1041–1061, doi:10.1175/1520-0469(2002)059<1041:NPOTNH>2.0.CO;2.

Hovan, S. A., D. K. Rea, and N. G. Pisias (1991), Late Pleistocene continental climate and oceanic variability recorded in northwest Pacific sediments, *Paleoceanography*, *6*, 349–370, doi:10.1029/91PA00559.

Jaccard, S. L., G. H. Haug, D. M. Sigman, T. F. Pedersen, H. R. Thierstein, and U. Röhl (2005), Glacial/interglacial changes in subarctic North Pacific stratification, *Science*, *308*(5724), 1003–1006, doi:10.1126/science.1108696.

Jaccard, S. L., E. D. Galbraith, D. M. Sigman, G. H. Haug, R. Francois, T. F. Pedersen, P. Dulski, and H. R. Thierstein (2009), Subarctic Pacific evidence for a glacial deepening of the oceanic respired carbon pool, *Earth Planet. Sci. Lett.*, *277*(1–2), 156–165, doi:10.1016/j.epsl.2008.10.017.

Jaccard, S. L., E. D. Galbraith, D. M. Sigman, and G. H. Haug (2010), A pervasive link between Antarctic ice core and subarctic Pacific sediment records, *Quat. Sci. Rev.*, *29*(1–2), 206–212, doi:10.1016/j.quascirev.2009.10.007.

Jiang, F. C., J. L. Fu, S. B. Wang, D. H. Sun, and Z. Z. Zhao (2007), Formation of the Yellow River, inferred from loess-palaeosol sequence in Mangshan and lacustrine sediments in Sanmen Gorge, China, *Quat. Int.*, *175*(1), 62–70, doi:10.1016/j.quaint.2007.03.022.

Jiang, X. Y., X. Y. Wang, Y. Q. He, H.-M. Hu, Z. Z. Li, C. Spötl, and C.-C. Shen (2016), Precisely dated multidecadally resolved Asian summer monsoon dynamics 113.5–86.8 thousand years ago, *Quat. Sci. Rev.*, *143*, 1–12, doi:10.1016/j.quascirev.2016.05.003.

Jickells, T. D., et al. (2005), Global iron connections between desert dust, ocean biogeochemistry, and climate, *Science*, *308*(5718), 67–71, doi:10.1126/science.1105959.

Kalnay, E., et al. (1996), The NCEP/NCAR 40-year reanalysis project, *Bull. Am. Meteorol. Soc.*, *77*(3), 437–471, doi:10.1175/1520-0477(1996)077<0437:TNYRP>2.0.CO;2.

Kang, S. G., H. M. Roberts, X. L. Wang, Z. S. An, and M. Wang (2015), Mass accumulation rate changes in Chinese loess during MIS 2, and asynchrony with records from Greenland ice cores and North Pacific Ocean sediments during the Last Glacial Maximum, *Aeol. Res.*, *19B*, 251–258, doi:10.1016/j.aeolia.2015.05.005.

Kapp, P., J. D. Pelletier, A. Rohrmann, R. Heermance, J. Russell, and L. Ding (2011), Wind erosion in the Qaidam basin, central China: Implications for tectonics, paleoclimate, and the source of the Loess Plateau, *Geol. Soc. Am. Today*, *21*(4–5), 4–10, doi:10.1130/GSATG99A.1.

Karabanov, E. B., A. A. Prokopenko, D. F. Williams, and S. M. Colman (1998), Evidence from Lake Baikal for Siberian glaciation during oxygen-isotope substage 5d, *Quat. Res.*, *50*(1), 46–55, doi:10.1006/qres.1998.1980.

Kaufman, Y. J., D. Tanré, and O. Boucher (2002), A satellite view of aerosols in the climate system, *Nature*, *419*(6903), 215–223, doi:10.1038/nature01091.

Kawahata, H., T. Okamoto, E. Matsumoto, and H. Ujiie (2000), Fluctuations of eolian flux and ocean productivity in the mid-latitude North Pacific during the last 200 kyr, *Quat. Sci. Rev.*, *19*(13), 1279–1291, doi:10.1016/S0277-3791(99)00096-7.

Keigwin, L. D. (1998), Glacial-age hydrography of the far northwest Pacific Ocean, *Paleoceanography*, *13*, 323–339, doi:10.1029/98PA00874.

Kienast, S. S., G. Winckler, J. Lippold, S. Albani, and N. M. Mahowald (2016), Tracing dust input to the global ocean using thorium isotopes in marine sediments: ThoroMap, *Global Biogeochem. Cycles*, *30*, 1526–1541, doi:10.1002/2016GB005408.

Kleman, J., K. Jansson, H. De Angelis, A. P. Stroeven, C. Hättestrand, G. Alm, and N. Glasser (2010), North American Ice Sheet build-up during the last glacial cycle, 115–21 kyr, *Quat. Sci. Rev.*, *29*(17–18), 2036–2051, doi:10.1016/j.quascirev.2010.04.021.

Kohfeld, K. E., and S. P. Harrison (2003), Glacial-interglacial changes in dust deposition on the Chinese Loess Plateau, *Quat. Sci. Rev.*, *22*(18–19), 1859–1878, doi:10.1016/S0277-3791(03)00166-5.

Krinner, G., B. Diekmann, F. Colleoni, and G. Stauch (2011), Global, regional and local scale factors determining glaciation extent in Eastern Siberia over the last 140,000 years, *Quat. Sci. Rev.*, *30*(7–8), 821–831, doi:10.1016/j.quascirev.2011.01.001.

Kurosaki, Y., and M. Mikami (2005), Regional difference in the characteristic of dust event in East Asia: Relationship among dust outbreak, surface wind, and land surface condition, *J. Meteorol. Soc. Jpn.*, *83A*, 1–18, doi:10.2151/jmsj.83A.1.

Li, G. Q., et al. (2016), Paleoenvironmental changes recorded in a luminescence dated loess/paleosol sequence from the Tianshan Mountains, arid central Asia, since the Penultimate Glaciation, *Earth Planet. Sci. Lett.*, *448*, 1–12, doi:10.1016/j.epsl.2016.05.008.

Licht, A., A. Pullen, P. Kapp, J. Abell, and N. Giesler (2016), Eolian cannibalism: Reworked loess and fluvial sediment as the main sources of the Chinese Loess Plateau, *Geol. Soc. Am. Bull.*, *128*(5–6), 944–956, doi:10.1130/B31375.1.

Liu, M., D. K. Westphal, S. G. Wang, A. Shimizu, N. Sugimoto, J. Zhou, and Y. Chen (2003), A high-resolution numerical study of the Asian dust storms of April 2001, *J. Geophys. Res.*, *108*(D23), 8653, doi:10.1029/2002JD003178.

Ma, Z. B., Z. H. Wang, J. Q. Liu, B. Y. Yuan, J. L. Xiao, and G. P. Zhang (2004), U-series chronology of sediments associated with Late Quaternary fluctuations, Balikun Lake, northwestern China, *Quat. Int.*, *121*(1), 89–98, doi:10.1016/j.quaint.2004.01.025.

Maher, B. A., T. J. Mutch, and D. Cunningham (2009), Magnetic and geochemical characteristics of Gobi Desert surface sediments: Implications for provenance of the Chinese Loess Plateau, *Geology*, *37*(3), 279–282, doi:10.1130/G25293A.1.

Marshall, S. J., T. S. James, and G. K. C. Clarke (2002), North American Ice Sheet reconstructions at the Last Glacial Maximum, *Quat. Sci. Rev.*, *21*(1–3), 175–192, doi:10.1016/S0277-3791(01)00089-0.

McGee, D., W. S. Broecker, and G. Winckler (2010), Gustiness: The driver of glacial dustiness?, *Quat. Sci. Rev.*, *29*(17–18), 2340–2350, doi:10.1016/j.quascirev.2010.06.009.

McGee, D., P. B. deMenocal, G. Winckler, J. B. W. Stuut, and L. I. Bradtmiller (2013), The magnitude, timing and abruptness of changes in North African dust deposition over the last 20,000 yr, *Earth Planet. Sci. Lett.*, *371–372*, 163–176, doi:10.1016/j.epsl.2013.03.054.

McGee, D., et al. (2016), Tracking eolian dust with helium and thorium: Impacts of grain size and provenance, *Geochim. Cosmochim. Acta*, *175*, 47–67, doi:10.1016/j.gca.2015.11.023.

Melles, M., et al. (2012), 2.8 million years of arctic climate change from Lake El'gygytgyn, NE Russia, *Science*, *337*(6092), 315–320, doi:10.1126/science.1222135.

Nagashima, K., R. Tada, H. Matsui, T. Irino, A. Tani, and S. Toyoda (2007), Orbital- and millenial-scale variations in Asian dust transport path to the Japan Sea, *Palaeogeogr. Palaeoclimatol. Palaeoecol.*, *247*(1–2), 144–161, doi:10.1016/j.palaeo.2006.11.027.

Nagashima, K., R. Tada, A. Tani, Y. B. Sun, Y. Isozaki, S. Toyoda, and H. Hasegawa (2011), Millennial-scale oscillations of the westerly jet path during the last glacial period, *J. Asian Earth Sci.*, *40*(6), 1214–1220, doi:10.1016/j.jseaes.2010.08.010.

Niu, J. S., et al. (2015), Loess Plateau storage of Northeastern Tibetan Plateau-derived Yellow River sediment, *Nat. Comm.*, *6*, 8511, doi:10.1038/ncomms9511.

Paillard, D., L. Labeyrie, and P. Yiou (1996), Macintosh Program performs time-series analysis, *Eos Trans. AGU*, *77*(39), 379, doi:10.1029/96EO00259.

Painter, T. H., J. S. Deems, J. Belnap, A. F. Hamlet, C. C. Landry, and B. Udall (2010), Response of Colorado River runoff to dust radiative forcing in snow, *Proc. Natl. Acad. Sci. U.S.A.*, *107*(40), 17,125–17,130, doi:10.1073/pnas.0913139107.

Patterson, D. B., K. A. Farley, and M. D. Norman (1999), ^{4}He as a tracer of continental dust: A 1.9 million year record of aeolian flux to the west equatorial Pacific Ocean, *Geochim. Cosmochim. Acta*, *63*(5), 615–625, doi:10.1016/S0016-7037(99)00077-0.

Peterson, L. C., and W. L. Prell (1985), Carbonate preservation and rates of climatic change: An 800 kyr record from the Indian Ocean, in *The Carbon Cycle and Atmospheric CO_2: Natural Variations Archaen to Present*, edited by E. T. Sundquist and W. S. Broecker, pp. 251–270, AGU, Washington, D. C.

Porter, S. C. (2001), Chinese loess record of monsoon climate during the last glacial-interglacial cycle, *Earth Sci. Rev.*, *54*(1–3), 115–128, doi:10.1016/S0012-8252(01)00043-5.

Porter, S. C., and Z. S. An (1995), Correlation between climate events in the North Atlantic and China during the last glaciation, *Nature*, *375*(6529), 305–308, doi:10.1038/375305a0.

Prins, M. A., M. Vriend, G. Nugteren, J. Vandenberghe, H. Y. Lu, H. B. Zheng, and G. J. Weltje (2007), Late Quaternary aeolian dust input variability on the Chinese Loess Plateau: Inferences from unmixing of loess grain-size records, *Quat. Sci. Rev.*, *26*(1–2), 230–242, doi:10.1016/j.quascirev.2006.07.002.

Prokopenko, A. A., E. B. Karabanov, D. F. Williams, M. I. Kuzmin, N. J. Shackleton, S. J. Crowhurst, J. A. Peck, A. N. Gvozdkov, and J. W. King (2001), Biogenic silica record of the Lake Baikal response to climatic forcing during the Brunhes, *Quat. Res.*, *55*(2), 123–132, doi:10.1006/qres.2000.2212.

Prokopenko, A. A., E. B. Karabanov, D. F. Williams, and G. K. Khursevich (2002), The stability and the abrupt ending of the last interglaciation in southeastern Siberia, *Quat. Res.*, *58*(1), 56–59, doi:10.1006/qres.2002.2329.

Prokopenko, A. A., L. A. Hinnov, D. F. Williams, and M. I. Kuzmin (2006), Orbital forcing of continental climate during the Pleistocene: A complete astronomically tuned climatic record from Lake Baikal, SE Siberia, *Quat. Sci. Rev.*, *25*(23–24), 3431–3457, doi:10.1016/j.quascirev.2006.10.002.

Pullen, A., P. Kapp, A. T. McCallister, H. Chang, G. E. Gehrels, C. N. Garzione, R. V. Heermance, and L. Ding (2011), Qaidam Basin and northern Tibetan Plateau as dust sources for the Chinese Loess Plateau and paleoclimatic implications, *Geology*, *39*(11), 1031–1034, doi:10.1130/G32296.1.

Qian, W. H., L. S. Quan, and S. Y. Shi (2002), Variations of the dust storm in China and its climatic control, *J. Clim.*, *15*(10), 1216–1229, doi:10.1175/1520-0442(2002)015<1216:VOTDSI>2.0.CO;2.

Qiang, M., L. Lang, and Z. Wang (2010), Do fine-grained components of loess indicate westerlies: Insights from observations of dust storm deposits at Lenghu (Qaidam Basin, China), *J. Arid Environ.*, *74*(10), 1232–1239, doi:10.1016/j.jaridenv.2010.06.002.

Roe, G. (2009), On the interpretation of Chinese loess as a paleoclimate indicator, *Quat. Res.*, *71*(2), 150–161, doi:10.1016/j.yqres.2008.09.004.

Sachs, J. P., and R. F. Anderson (2005), Increased productivity in the subantarctic ocean during Heinrich events, *Nature*, *434*(7037), 1118–1121, doi:10.1038/nature03544.

Sahsamanoglou, H. S., T. J. Makrogiannis, and P. P. Kallimopoulos (1991), Some aspects of the basic characteristics of the Siberian anticyclone, *Int. J. Climatol.*, *11*(8), 827–839, doi:10.1002/joc.3370110803.

Sampe, T., and S. P. Xie (2010), Large-scale dynamics of the Meiyu-Baiu rainband: Environmental forcing by the westerly jet, *J. Clim.*, *23*(1), 113–134, doi:10.1175/2009JCLI3128.1.

Schiemann, R., D. Lüthi, and C. Schär (2009), Seasonality and interannual variability of the westerly jet in the Tibetan Plateau region, *J. Clim.*, *22*(11), 2940–2957, doi:10.1175/2008JCLI2625.1.

Serno, S., G. Winckler, R. F. Anderson, C. T. Hayes, D. McGee, B. Machalett, H. Ren, S. M. Straub, R. Gersonde, and G. H. Haug (2014), Eolian dust input to the Subarctic North Pacific, *Earth Planet. Sci. Lett.*, *387*, 252–263, doi:10.1016/j.epsl.2013.11.008.

Serno, S., G. Winckler, R. F. Anderson, E. Maier, H. Ren, R. Gersonde, and G. H. Haug (2015), Comparing dust flux records from the Subarctic North Pacific and Greenland: Implications for atmospheric transport to Greenland and for the application of dust as a chronostratigraphic tool, *Paleoceanography*, *30*, 583–600, doi:10.1002/2014PA002748.

Shigemitsu, M., H. Narita, Y. W. Watanabe, N. Harada, and S. Tsunogai (2007), Ba, Si, U, Al, Sc, La, Th, C and $^{13}C/^{12}C$ in a sediment core in the western subarctic Pacific as proxies of past biological production, *Mar. Chem.*, *106*(3–4), 442–455, doi:10.1016/j.marchem.2007.04.004.

Siddall, M., E. J. Rohling, A. Almogi-Labin, C. Hemleben, D. Meischner, I. Schmelzer, and D. A. Smeed (2003), Sea-level fluctuations during the last glacial cycle, *Nature*, *423*(6942), 853–858, doi:10.1038/nature01690.

Spratt, R. M., and L. E. Lisiecki (2016), A Late Pleistocene sea level stack, *Clim. Past*, *12*, 1079–1092, doi:10.5194/cp-12-1079-2016.

Stauch, G., and L. Gualtieri (2008), Late Quaternary glaciations in Northeastern Russia, *J. Quat. Sci.*, *23*(6–7), 545–558, doi:10.1002/jqs.1211.

Stevens, T., and H. Y. Lu (2009), Optically stimulated luminescence dating as a tool for calculating sedimentation rates in Chinese loess: Comparisons with grain-size records, *Sedimentology*, *56*(4), 911–934, doi:10.1111/j.1365-3091.2008.01004.x.

Stevens, T., S. J. Armitage, H. Y. Lu, and D. S. G. Thomas (2006), Sedimentation and diagenesis of Chinese loess: Implications for the preservation of continuous, high-resolution climate records, *Geology*, *34*(10), 849–852, doi:10.1130/G22472.1.

Stevens, T., G. Adamiec, A. F. Bird, and H. Y. Lu (2013), An abrupt shift in dust source on the Chinese Loess Plateau revealed through high sampling resolution OSL dating, *Quat. Sci. Rev.*, *82*, 121–132, doi:10.1016/j.quascirev.2013.10.014.

Sun, D. H., F. H. Chen, J. Bloemendal, and R. X. Su (2003), Seasonal variability of modern dust over the Loess Plateau of China, *J. Geophys. Res.*, *108*(D21), 4665, doi:10.1029/2003JD003382.

Sun, J. M., M. Y. Zhang, and T. S. Liu (2001), Spatial and temporal characteristics of dust storms in China and its surrounding regions, 1960–1999: Relations to source area and climate, *J. Geophys. Res.*, *106*, 10,325–10,333, doi:10.1029/2000JD900665.

Sun, Y. B., J. Chen, S. C. Clemens, Q. S. Liu, J. F. Ji, and R. Tada (2006), East Asian monsoon variability over the last seven glacial cycles recorded by a loess sequence from the northwestern Chinese Loess Plateau, *Geochem. Geophys. Geosyst.*, *7*, Q12Q02, doi:10.1029/2006GC001287.

Sun, Y. B., R. Tada, J. Chen, Q. S. Liu, S. Toyoda, A. Tani, J. F. Ji, and Y. Isozaki (2008), Tracing the provenance of fine-grained dust deposited on the central Chinese Loess Plateau, *Geophys. Res. Lett.*, *35*, L01804, doi:10.1029/2007GL031672.

Svendsen, J. I., et al. (2004), Late Quaternary ice sheet history of northern Eurasia, *Quat. Sci. Rev.*, *23*(11–13), 1229–1271, doi:10.1016/j.quascirev.2003.12.008.

Tegen, I., and I. Fung (1994), Modeling of mineral dust in the atmosphere: Sources, transport, and optical thickness, *J. Geophys. Res.*, *99*, 22,897–22,914, doi:10.1029/94JD01928.

Thompson, L. G., T. D. Yao, M. E. Davis, K. A. Henderson, E. Mosley- Thompson, P.-N. Lin, J. Beer, H.-A. Synal, J. Cole-Dai, and J. F. Bolzan (1997), Tropical climate instability: The last glacial cycle from a Qinghai-Tibetan ice core, *Science*, *276*(5320), 1821–1825, doi:10.1126/science.276.5320.1821.

Waelbroeck, C., L. Labeyrie, E. Michel, J. C. Duplessy, J. F. McManus, K. Lambeck, E. Balbon, and M. Labracherie (2002), Sea-level and deep water temperature changes derived from benthic foraminifera isotopic records, *Quat. Sci. Rev.*, *21*(1–3), 295–305, doi:10.1016/S0277-3791(01)00101-9.

Wallace, J. M., and P. V. Hobbs (2006), *Atmospheric Science: An Introductory Survey*, 2nd ed., Academic Press, San Diego, Calif.

Wang, Y. J., H. Cheng, R. L. Edwards, X. G. Kong, X. H. Shao, S. T. Chen, J. Y. Wu, X. Y. Jiang, X. F. Wang, and Z. S. An (2008), Millennial- and orbital-scale changes in the East Asian monsoon over the past 224,000 years, *Nature*, *451*(7182), 1090–1093, doi:10.1038/nature06692.

Winckler, G., R. F. Anderson, and P. Schlosser (2005), Equatorial Pacific productivity and dust flux during the mid-Pleistocene climate transition, *Paleoceanography*, *20*, PA4025, doi:10.1029/2005PA001177.

Winckler, G., R. F. Anderson, M. Q. Fleisher, D. McGee, and N. Mahowald (2008), Covariant glacial-interglacial dust fluxes in the Equatorial Pacific and Antarctica, *Science*, *320*(5872), 93–96, doi:10.1126/science.1150595.

Xiao, J. L., Z. S. An, T. S. Liu, Y. Inouchi, H. Kumai, S. Yoshikawa, and Y. Kondo (1999), East Asian monsoon variation during the last 130,000 Years: Evidence from the Loess Plateau of central China and Lake Biwa of Japan, *Quat. Sci. Rev.*, *18*(1), 147–157, doi:10.1016/S0277-3791(97)00097-8.

Yang, M. X., T. D. Yao, H. J. Wang, and X. H. Gou (2006), Climatic oscillations over the past 120 kyr recorded in the Guliya ice core, China, *Quat. Int.*, *154–155*, 11–18, doi:10.1016/j.quaint.2006.02.015.

Yang, S. L., S. L. Forman, Y. G. Song, J. Pierson, J. Mazzocco, X. X. Li, Z. T. Shi, and X. M. Fang (2014), Evaluating OSL-SAR protocols for dating quartz grains from the loess in Ili Basin, Central Asia, *Quat. Geochron.*, *20*, 78–88, doi:10.1016/j.quageo.2013.11.004.

Yang, X. P., L. Scuderi, P. Paillou, Z. T. Liu, H. W. Li, and X. Z. Ren (2011), Quaternary environmental changes in the drylands of China—A critical review, *Quat. Sci. Rev.*, *30*(23–24), 3219–3233, doi:10.1016/j.quascirev.2011.08.009.

Yao, T. D., L. G. Thompson, Y. F. Shi, D. H. Qin, K. Q. Jiao, Z. H. Yang, L. D. Tian, and E. Mosley-Thompson (1997), Climate variation since the Last Interglaciation recorded in the Guliya ice core, *Sci. China Ser. D*, *40*(6), 662–668, doi:10.1007/BF02877697.

Zech, W., R. Zech, M. Zech, K. Leiber, M. Dippold, M. Frechen, R. Bussert, and A. Andreev (2011), Obliquity forcing of Quaternary glaciation and environmental changes in NE Siberia, *Quat. Int.*, *234*(1–2), 133–145, doi:10.1016/j.quaint.2010.04.016.